World Journal of Surgical Oncology

RESEARCH

Open Access

Predicting postoperative recurrence and survival in glioma patients using enhanced MRI-based delta habitat radiomics: an 8-year retrospective pilot study

Xiumei Li[1,2†], Lina Song[1,2†], Haidong Zhang[1†], Xianqun Ji[1,2], Ping Song[1], Junjie Liu[1,2*] and Peng An[1,2*]

Abstract

Objective This study aimed to develop predictive models for postoperative recurrence and overall survival in patients with brain glioma (BG) by integrating preoperative contrast-enhanced MRI-derived delta habitat radiomics features with clinical characteristics.

Methods In this retrospective study, preoperative contrast-enhanced MRI data and clinical records of 187 BG patients were analyzed. Patients were stratified into non-recurrence ($n=100$) and recurrence ($n=87$) cohorts based on postoperative outcomes. The dataset was randomly divided into training and test sets (7:3 ratio). Delta habitat radiomic features were extracted from intratumoral and peritumoral edema regions. A radiomic score (Radscore) was generated via LASSO regression with ten-fold cross-validation in the training cohort. Clinical variables (gender, IDH1 mutation, 1p19q co-deletion, MRI enhancement patterns) and radiomic features were compared between groups using χ^2 or Student's t-tests. Multivariate logistic regression models incorporating significant predictors were developed. Model performance was evaluated using AUC comparisons (DeLong test), decision curve analysis (clinical utility), and validated via XGBoost machine learning. Nomograms were constructed to visualize recurrence and survival predictions.

Results The training cohort revealed significant intergroup differences in gender, IDH1 mutation, 1p19q co-deletion, MRI enhancement patterns, and delta habitat radiomic scores (Radscore1/2, $p<0.05$). The combined model (clinical + radiomic features) demonstrated superior predictive performance for recurrence [AUC 0.921 (95% CI 0.861–0.961), OR 0.023, sensitivity: 87.18%, specificity: 82.03%] compared to clinical-only [AUC 0.802 (0.745–0.833), OR 0.036] and radiomic-only [AUC 0.843 (0.769–0.900), OR 0.034] models ($p<0.05$, DeLong test). Decision curve analysis confirmed greater clinical net benefit for the combined model. These findings were replicated in the test cohort. The

†Xiumei Li, Lina Song and Haidong Zhang contributed equally to this work.

*Correspondence:
Junjie Liu
liujj2023@yeah.net
Peng An
drpengan@foxmail.com

Full list of author information is available at the end of the article

survival nomogram incorporated IDH1 mutation status, gender, and Radscore1/2, with Kaplan-Meier analysis verifying their prognostic significance ($p < 0.01$).

Conclusion Delta habitat radiomics derived from preoperative contrast-enhanced MRI may enhance the accuracy of postoperative recurrence and survival predictions in BG patients. The validated nomograms provide actionable tools for optimizing postoperative surveillance and personalized clinical decision-making.

Keywords Delta habitat radiomics, Glioma prognosis, MRI radiomics, Machine learning, XGBoost, Contrast-enhanced MRI, Survival prediction

Introduction

Brain gliomas (BGs), the most prevalent primary intracranial malignancies in adults, are characterized by aggressive biological behavior, high recurrence rates, and poor clinical outcomes. In China, the incidence of BG has risen to 5–8 cases per 100,000 population annually, driven by environmental factors, genetic mutations, and improved diagnostic capabilities [1–3]. Despite multimodal therapies—including maximal safe resection followed by radiotherapy and temozolomide-based chemotherapy—the prognosis remains dismal, with a median overall survival (OS) of 22.5 months and a five-year survival rate of merely 7.2%. Postoperative recurrence, a critical determinant of survival, imposes substantial psychological and socioeconomic burdens on patients due to repeated imaging surveillance and therapeutic interventions. Contrast-enhanced MRI (CE-MRI) remains the cornerstone for BG diagnosis and monitoring. However, conventional MRI lacks the sensitivity to predict early recurrence or quantify tumor microenvironment heterogeneity, which underpins therapeutic resistance and progression [4–6]. Radiomics, an advanced computational tool, addresses this gap by extracting high-dimensional imaging features that reflect tumor biology beyond human visual perception. While existing radiomic studies have focused on static enhancement characteristics of tumors during specific imaging phases (e.g., Non-Contrast Phase, Arterial Phase, or Venous Phase), they often neglect peritumoral microenvironment dynamics and temporal evolution of recurrence risk [7–9]. Unlike conventional static radiomics approaches that analyze single-timepoint enhancement patterns, our delta habitat radiomics framework dynamically quantifies spatial-temporal heterogeneity across intratumoral and peritumoral habitats. This method captures microenvironmental interactions critical for recurrence, a dimension overlooked in prior studies focused solely on tumor core features. By combining these features with clinicopathological variables, we aim to develop prognostic tools to optimize postoperative management and personalized therapeutic strategies (Fig. 1).

Methods

Study population

This retrospective cohort study included 234 patients with histopathologically confirmed BG treated at our institution between August 2015 and April 2023. Inclusion criteria were: (1) Standard tumor resection (neuroendoscopic or open craniotomy) with postoperative BG diagnosis; (2) Preoperative CE-MRI within one month prior to surgery; (3) Completion of adjuvant radiotherapy and temozolomide chemotherapy; (4) Minimum three-year follow-up data. Exclusion criteria comprised: (1) Poor MRI quality (motion artifacts, incomplete sequences); (2) Incomplete clinical/imaging records; (3) Prior glioma recurrence, concurrent malignancies, or contraindications to MRI contrast agents; (4) Impaired liver or kidney function, or claustrophobia. After exclusions, 187 patients were analyzed. Based on Response Assessment in Neuro-Oncology (RANO) criteria, patients were stratified into non-recurrence ($n = 100$) and recurrence ($n = 87$) cohorts. The dataset was partitioned into training (70%) and test (30%) sets using time-stratified randomized sampling to mitigate temporal bias (Fig. 2). Demographic and clinicopathological variables included: Age, gender, WHO tumor grade (2021 CNS5 classification); Molecular markers: IDH1 mutation, 1p19q co-deletion, MGMT promoter methylation (methylation-specific PCR), Ki-67 index (immunohistochemistry); Comorbidities: diabetes, hypertension; Lifestyle factors: smoking, alcohol use. Ethical Approval: The study protocol was approved by the Institutional Ethics Committee of Xiangyang No.1 People's Hospital affiliated with Hubei University of Medicine (Approval No.: XYYYE20240011). Written informed consent was obtained from all participants or legal guardians [10–11].

MRI acquisition and radiomics workflow

Imaging Protocol: Preoperative cranial MRI was performed using 3.0T scanners (Philips Ingenia and Siemens MAGNETOM Vida) equipped with 8-channel head coils. The protocol included: Non-contrast sequences: Axial T1-weighted imaging (T1WI), T2-weighted imaging (T2WI), T2 fluid-attenuated inversion recovery (T2 FLAIR), diffusion-weighted imaging (DWI), and apparent diffusion coefficient (ADC) mapping. Post-contrast

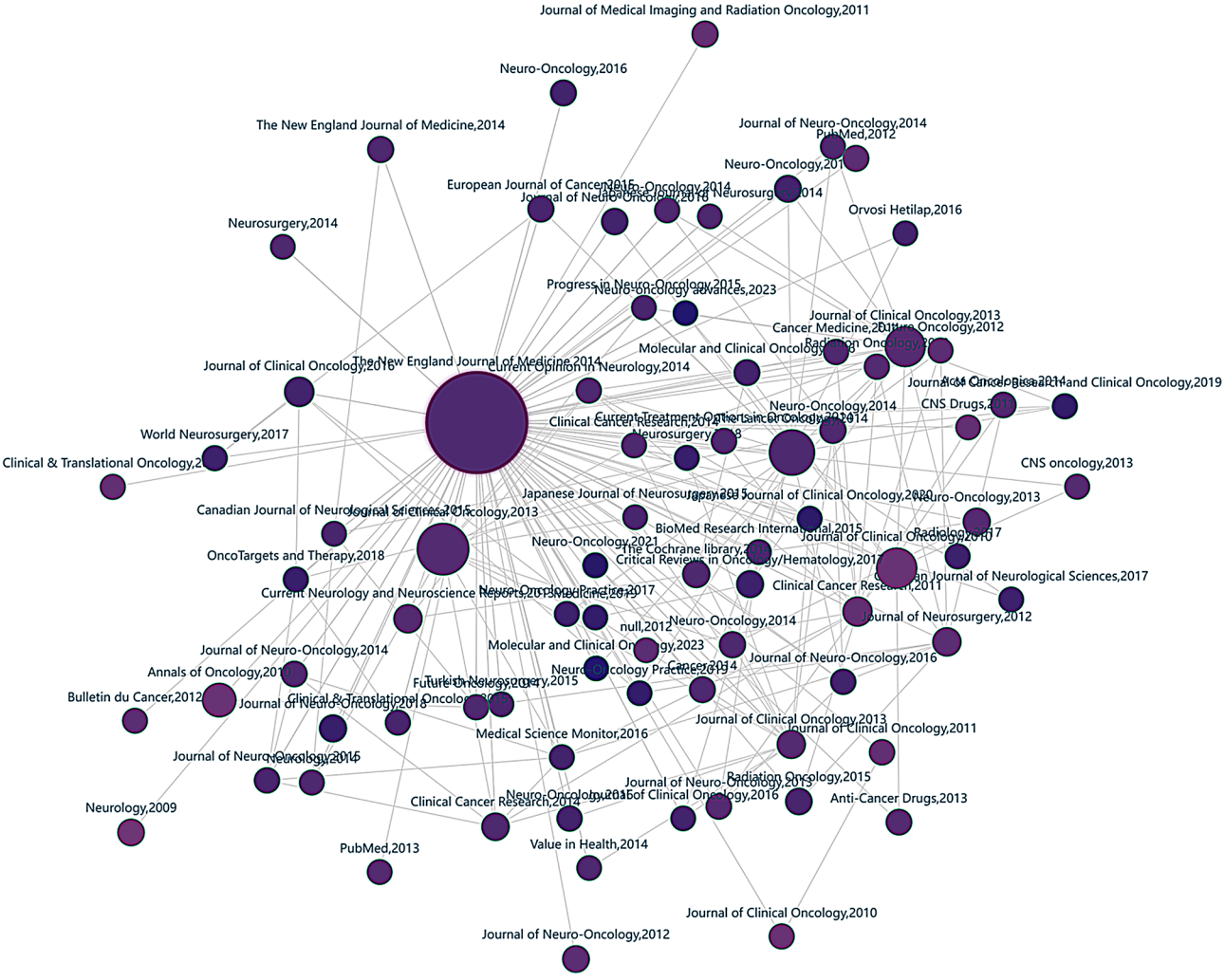

Fig. 1 According to Web of Science, recent research hotspots on glioma have focused on molecular mechanisms, radiotherapy and chemotherapy, and animal models. There were relatively rare reports on using delta habitat radiomics data derived from enhanced MR imaging to predict recurrence and overall survival

sequences: T1WI with gadopentetate dimeglumine (0.1 mmol/kg IV). Enhanced T1WI parameters: matrix size 256 × 256, slice thickness 1/5 mm, field of view (FOV) 240 × 240 mm^2, repetition time (TR) 1820 ms, echo time (TE) 30 ms, and 1 excitation. N4 bias correction and ComBat harmonization were applied to minimize scanner variability. Intensity normalization used histogram matching to a reference scan, ensuring feature stability across acquisition parameters. Region of Interest (ROI) Segmentation: Two blinded observers (a neuroradiologist with 12 years' experience and an MR technician with 8 years' experience) independently delineated ROIs on post-contrast T1WI images using 3D Slicer (v4.13): (1) Intratumoral region: Enhancing tumor core. (2) Peritumoral habitat: 3–12 mm margin surrounding the tumor, guided by CNS tumor imaging consensus guidelines. Each observer performed segmentations twice to assess inter-/intra-rater reliability via intraclass correlation coefficient (ICC > 0.75 threshold for stability).Two staffs independently segmented ROIs. Intraclass correlation coefficients (ICC) for inter-/intra-observer agreement exceeded 0.85 for 94% of features. Discordant segmentations (< 5%) were resolved by consensus. Radiomic Feature Extraction and Processing: (1) Preprocessing: Isotropic resampling (1 × 1 × 1 mm^3 voxels). Z-score normalization of feature values. (2) Feature extraction: 870 radiomic features per sequence, including: First-order statistics, 3D shape descriptors. Texture matrices: gray-level co-occurrence matrix (GLCM), gray-level dependence matrix (GLDM), gray-level run-length matrix (GLRLM), gray-level size zone matrix (GLSZM), neighborhood gray-tone difference matrix (NGTDM). Transformed features: Wavelet decompositions, Laplacian of Gaussian. (3) Delta habitat radiomics: Δ-features = (Enhanced feature value) – (Non-enhanced feature value). Radscore1: Peritumoral habitat (3–12 mm

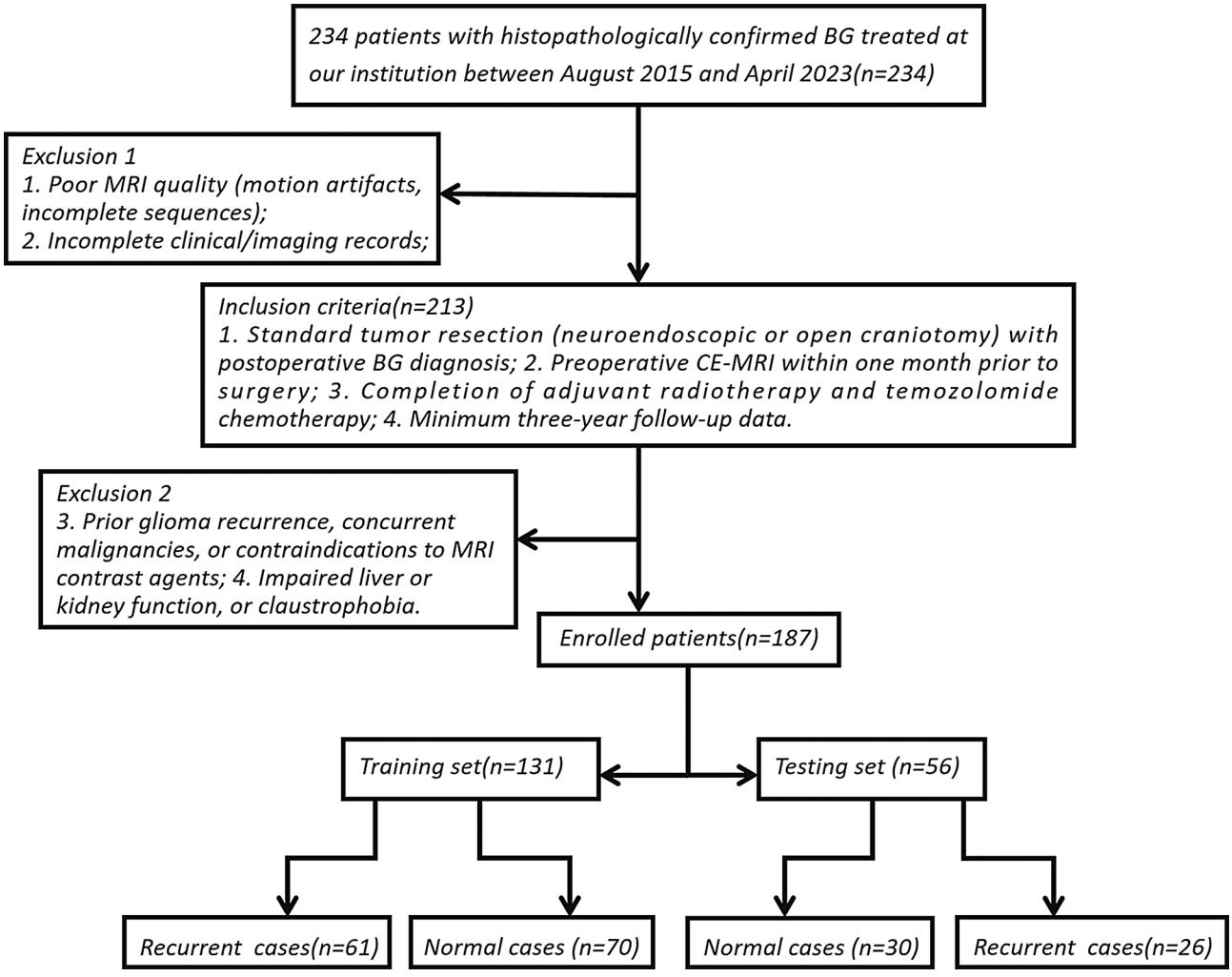

Fig. 2 Schematic diagram of case registration and grouping in this study

margin). Radscore2: Intratumoral region (Fig. 3). Feature Selection: 1.Stability filtering: Retained features with ICC > 0.75. 2.Dimensionality reduction: Minimum redundancy maximum relevance (MRMR) for initial selection. LASSO regression with 10-fold cross-validation (λ optimized via minimum mean squared error) to derive final radiomic signatures and corresponding radscores [12–13].

Statistical analysis

All analyses were performed using R software (version 4.3.1; R Foundation for Statistical Computing). Feature selection and model development followed a staged approach: (1) Minimum Redundancy Maximum Relevance (MRMR): Implemented via the `mRMRe` package to prioritize radiomic features with high discriminative power and low redundancy. (2) LASSO Regression: Applied using the `glmnet` package with 10-fold cross-validation to optimize regularization (λ selected by minimum mean squared error), generating radiomic scores (Radscore1/2). Group Comparisons - Categorical variables: Assessed by χ^2 or Fisher's exact tests (cell counts < 5). Continuous variables: Normality evaluated via Shapiro-Wilk test; parametric comparisons used independent t-tests, while nonparametric data employed Wilcoxon rank-sum tests. Significance threshold: Two-tailed $P < 0.05$. Model Construction and Validation: 1.Training Cohort: Clinicopathological model: Clinically significant predictors (e.g., IDH1 status, 1p19q co-deletion). Imaging model: Radscore1 (peritumoral) and Radscore2 (intratumoral). Combined model: Integration of clinicopathological and radiomic features. 2. Performance Metrics: ROC curves (`pROC` package) with DeLong test for AUC comparisons. Decision curve analysis (DCA) to quantify clinical utility across risk thresholds. XGBoost validation (Python 3.9, `xgboost` package; hyperparameters tuned via grid search). XGBoost was chosen for its robustness to class imbalance and ability to model non-linear interactions. Moreover, its SHAP-based visualization of feature importance provides an excellent validation of the

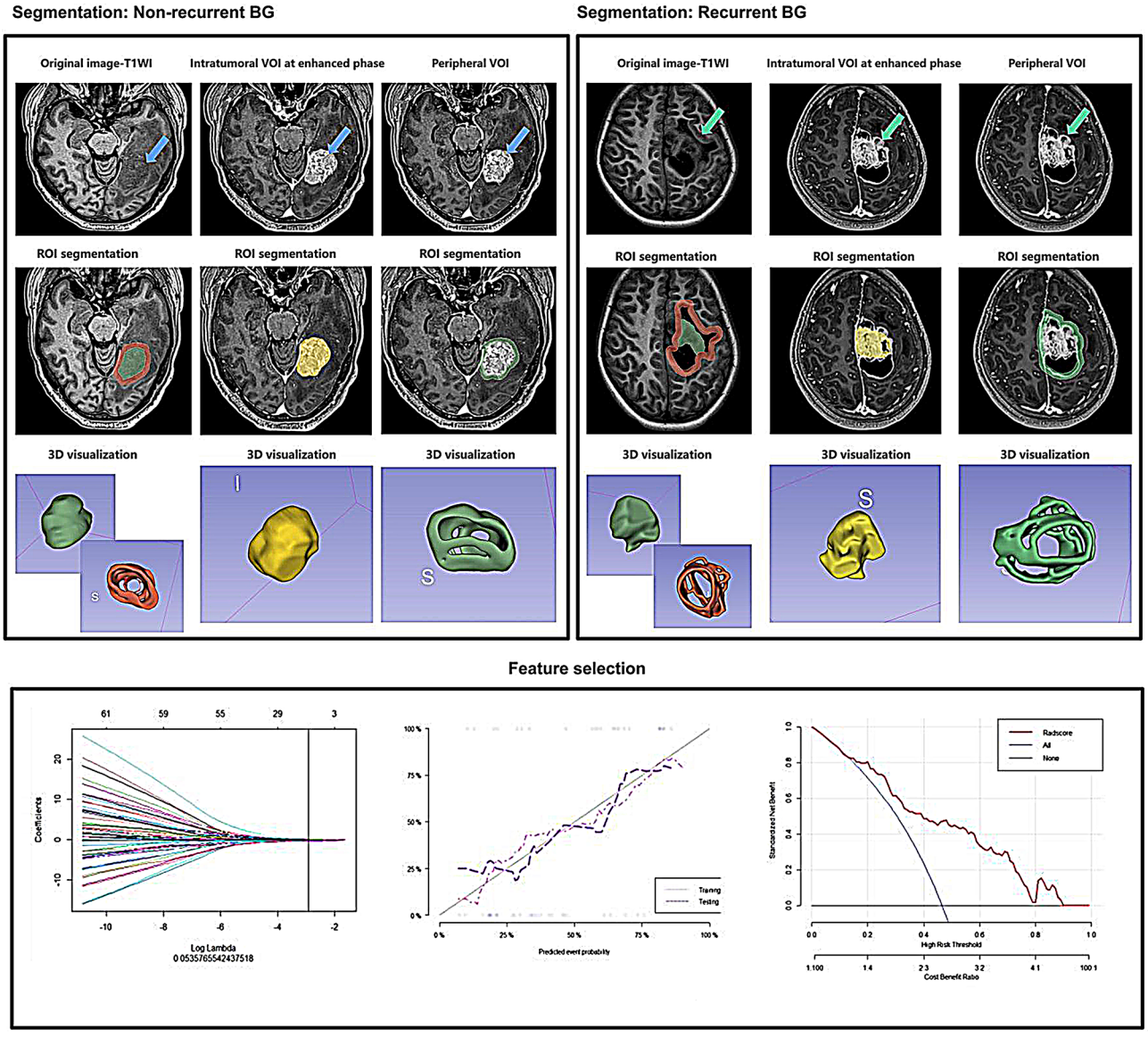

Fig. 3 The flowchart for extracting and generating contrast-enhanced magnetic resonance radiomics(Delta habitat radscore) in this study

predictive factors in the combined model, outperforming those of the SVM and Random Forest models.3. Test Cohort: Model generalizability assessed using locked coefficients from the training phase. Nomogram Development Multivariable logistic regression results were visualized as nomograms using the `rms` package, with calibration curves and Brier scores evaluating prediction accuracy [14, 15].

Results

Baseline characteristics

No significant differences were observed between recurrence and non-recurrence groups in age, Ki-67 expression, MGMT promoter methylation status, diabetes/hypertension history, or smoking/alcohol use ($P > 0.05$; Tables 1 and 2). Significant intergroup disparities were identified in gender, IDH1 mutation status, 1p19q co-deletion frequency, and MRI enhancement patterns ($P < 0.05$).

Radiomic feature selection

Of 870 initially extracted radiomic features, 851 (94.1%) demonstrated high interobserver reproducibility (ICC > 0.75). Subsequent MRMR filtering and LASSO regression with 10-fold cross-validation yielded two delta habitat radiomic signatures: Radscore1 (peritumoral habitat): Incorporated 10 features (e.g., Maximum2DDiameterColumn, ClusterShade, Imc1;). Radscore2(intratumoral region): Included 5 features(e.g., GrayLevelNonUniformity,

Table 1 Comparison results of clinical and imaging data between the two groups

Factors	Normal group ($n=100$)	Recurrence group($n=87$)	X^2, Z or t value	*P*
Hypertension history	18.24 ± 15.09	14.89 ± 13.59	1.58	0.12
Diabetes history	8.11 ± 3.86	9.76 ± 5.62	1.34	0.18
Smoking history	17.48 ± 15.49	18.81(0,28.12)	0.59	0.56
Drinking history	22.75 ± 20.39	27.50 ± 17.29	1.70	0.09
Age	55.13 ± 7.01	54.34 ± 7.97	0.72	0.48
MGMT promoter methylation			0.60	0.44
1(No)	73	59		
2(Yes)	27	28		
BMI	25.03(22.02,26.70)	24.53 ± 2.96	1.19	0.24
Tumor location			1.82	0.07
1(fronto-parietal lobe)	55	38		
2(The temporal lobe and basal ganglia region)	23	20		
3(Cerebellum and occipital lobe)	22	29		
WHO grade			1.85	0.07
1 stage	61	41		
2 stage	18	20		
3 stage	21	26		
Ki67	33.12 ± 17.34	38.19 ± 18.93	1.91	0.06
Surgical method			0.12	0.73
1(craniotomy)	76	68		
2(Da Vinci + neuroendoscope)	24	19		
Gender			35.03	< 0.05*
Male	84	37		
Female	16	50		
Radscore 1	0.44 ± 0.08	0.49 ± 0.06	4.95	< 0.05*
Radscore 2	0.38 ± 0.13	0.55 ± 0.15	8.18	< 0.05*
MR enhancement patterns			2.72	< 0.05*
1(Inflow type)	7	16		
2(Plateau type)	25	26		
3(Outflow type)	68	45		
IDH1 mutation			7.53	0.01*
0(Yes)	67	41		
1(No)	33	46		
1p19q co-deletion			8.04	< 0.05*
0(Yes)	87	61		
1(No)	13	26		
Local tumor necrosis			1.47	0.22
0(No)	65	49		
1(Yes)	35	38		
PLR	142.28 ± 42.51	154.03 ± 51.53	1.71	0.09
NLR	3.68(2.39,3.95)	4.08 ± 1.51	1.84	0.07

P-value < 0.05* indicates statistical significance, with significant differences observed between the two groups in terms of gender, IDH1 mutations, 1p19q co-deletion, Radscore 1/2, and enhancement patterns on contrast-enhanced MR imaging. PLR: Platelet to Lymphocyte Ratio, NLR: Neutrophil to Lymphocyte Ratio

SizeZoneNonUniformityNormalized;). Both scores differed significantly between recurrence and non-recurrence cohorts ($P < 0.05$; Table 3).

Model performance

In the training cohort, the combined model (clinicopathological + radiomic features) outperformed standalone models: Combined model: AUC 0.921 (95% CI 0.861–0.961), sensitivity: 87.18%, specificity: 82.03%, Precision: 80.30%, OR 0.023. VS. Clinicopathological model: AUC 0.802 (0.745–0.833), OR 0.036. VS. Imaging model: AUC 0.843 (0.769–0.900), OR 0.034 (Table 4; Fig. 4). XGBoost validation confirmed the combined model's robustness, while decision curve analysis demonstrated superior clinical net benefit across risk thresholds (Figs. 5, 6 and 7). Test cohort validation replicated these findings: Combined model: AUC 0.891 (0.779–0.959), sensitivity: 83.33%, specificity: 80.81%, Precision: 79.02%,OR 0.045.

Table 2 Results of logistic regression analysis for predicting BG recurrence based on clinicopathological data from two groups, *$P < 0.05$

Clinicopathological model	Univariate analysis		Multivariate analysis	
factors	***P***	**Hazard ratio**	***P***	**Hazard ratio**
Hypertension history	0.18	0.98(0.96–1.01)		
Diabetes history	0.45	1.01(0.97–1.05)		
Smoking history	0.57	1.01(0.98–1.03)		
Drinking history	0.08	1.02(0.99–1.04)		
Age	0.11	0.96(0.92–1.01)		
MGMT promoter methylation	0.76	1.12(0.53–2.41)		
BMI	0.09	0.89(0.79–1.02)		
Tumor location	0.12	1.36(0.92–2.02)		
WHO grade	0.11	1.38(0.93–2.06)		
Ki67	0.09	1.02(0.99–1.04)		
Surgical method	0.55	1.19(0.67–2.10)		
Gender	< 0.05*	9.91(4.25–23.11)	< 0.05*	15.96(5.85–43.49)
IDH1 mutation	0.03*	2.12(1.05–4.28)	< 0.05*	4.45(1.73–11.42)
1p19q co-deletion	0.03*	2.51(1.06–5.97)	0.04*	3.08(1.07–8.91)
Local tumor necrosis	0.61	1.20(0.60–2.40)		
PLR	0.12	1.01(0.99–1.10)		
NLR	0.22	1.16(0.92–1.46)		

P-value < 0.05* indicates statistical significance, In clinicopathological model, multivariate analysis has confirmed that gender, IDH1 mutation and 1p19q co-deletion were independent predictors of BG recurrence.PLR: Platelet to Lymphocyte Ratio, NLR: Neutrophil to Lymphocyte Ratio

Table 3 Results of logistic regression analysis for predicting BG recurrence based on imaging data from two groups, *$P < 0.05$

Imaging Model	Univariate analysis		Multivariate analysis	
factors	***P***	**Hazard ratio**	***P***	**Hazard ratio**
Radscore 1	< 0.05*	3.73(1.95–7.13)	< 0.05*	2.57(1.27–5.19)
Radscore 2	< 0.05*	2.15(1.64–2.81)	< 0.05*	1.95(1.48–2.58)
MR enhancement patterns	0.04*	1.65(1.01–2.69)		

P-value < 0.05* indicates statistical significance, In imaging model, multivariate analysis has confirmed that Radscore 1, and Radscore 2 were independent predictors of BG recurrence

Table 4 Results of logistic regression analysis for predicting BG recurrence based on clinicopathological imaging data from two groups, *$P < 0.05$

Combined Model	Univariate analysis		Multivariate analysis	
factors	***P***	**Hazard ratio**	***P***	**Hazard ratio**
Gender	< 0.05*	9.91(4.25–23.11)	< 0.05*	45.32(9.53-215.53)
IDH1 mutation	0.03*	2.12(1.05–4.28)	< 0.05*	7.19(1.98–26.06)
1p19q co-deletion	0.03*	2.51(1.06–5.97)		
Radscore 1	< 0.05*	3.73(1.95–7.13)	< 0.05*	6.22(2.29–16.89)
Radscore 2	< 0.05*	2.15(1.64–2.81)	< 0.05*	1.81(1.25–2.60)
MR enhancement patterns	0.04*	1.65(1.01–2.69)		

P-value < 0.05* indicates statistical significance, In combined model, multivariate analysis has confirmed that gender, IDH1 mutation and Radscore 1/2 were independent predictors of BG recurrence

VS. Clinicopathological model: AUC 0.743 (0.609–0.850), OR 0.066. VS. Imaging model: AUC 0.827 (0.702–0.915), OR 0.056. The nomogram developed through the combined model significantly streamlines the prediction workflow for BG recurrence.

Survival analysis

Kaplan-Meier analysis identified IDH1 mutation status, gender, and Radscore1/2 ($P < 0.05$) as independent prognostic factors for overall survival. The survival nomogram integrating these predictors demonstrated clinically meaningful calibration (Brier score 0.13) and discrimination (C-index 0.81) (Table 5; Figs. 8, 9 and 10).

Discussion

The diagnostic accuracy of brain gliomas (BG) has significantly improved with the widespread adoption of advanced CT and MRI screening technologies, enabling timely clinical interventions and substantially enhancing patients' quality of life compared to previous decades.

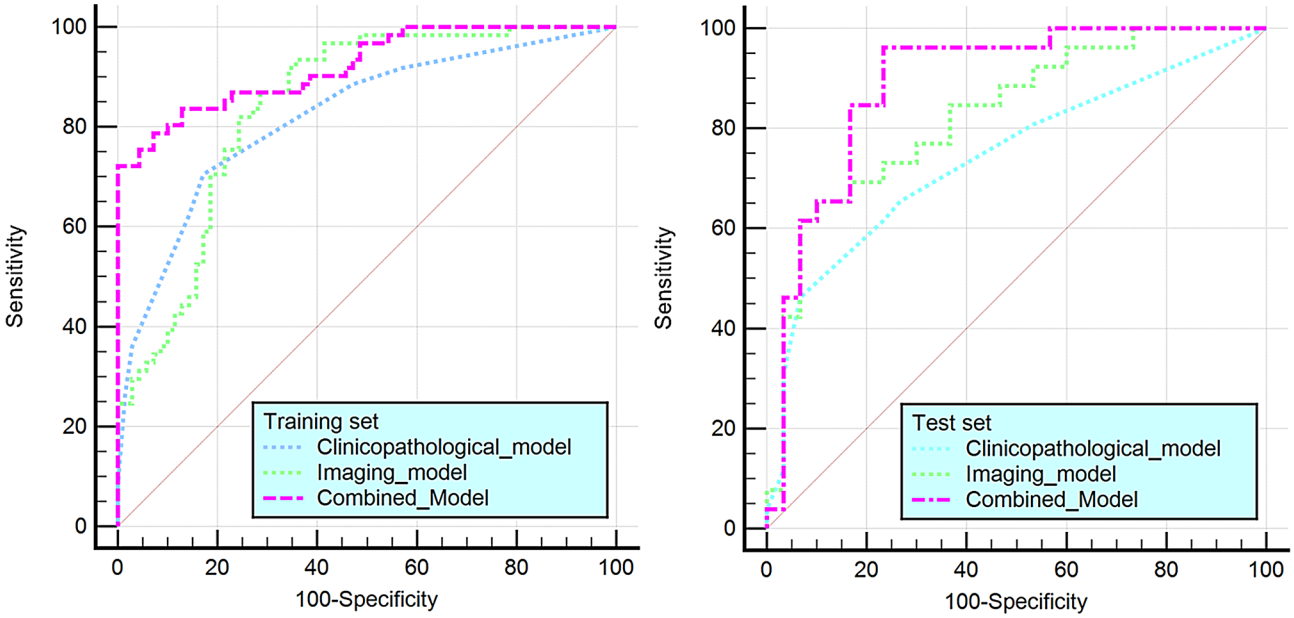

Fig. 4 All models in this study were compared using DeLong's curve, and the combined model demonstrated strong predictive performance in both the training set (left figure) and the test set (right figure)

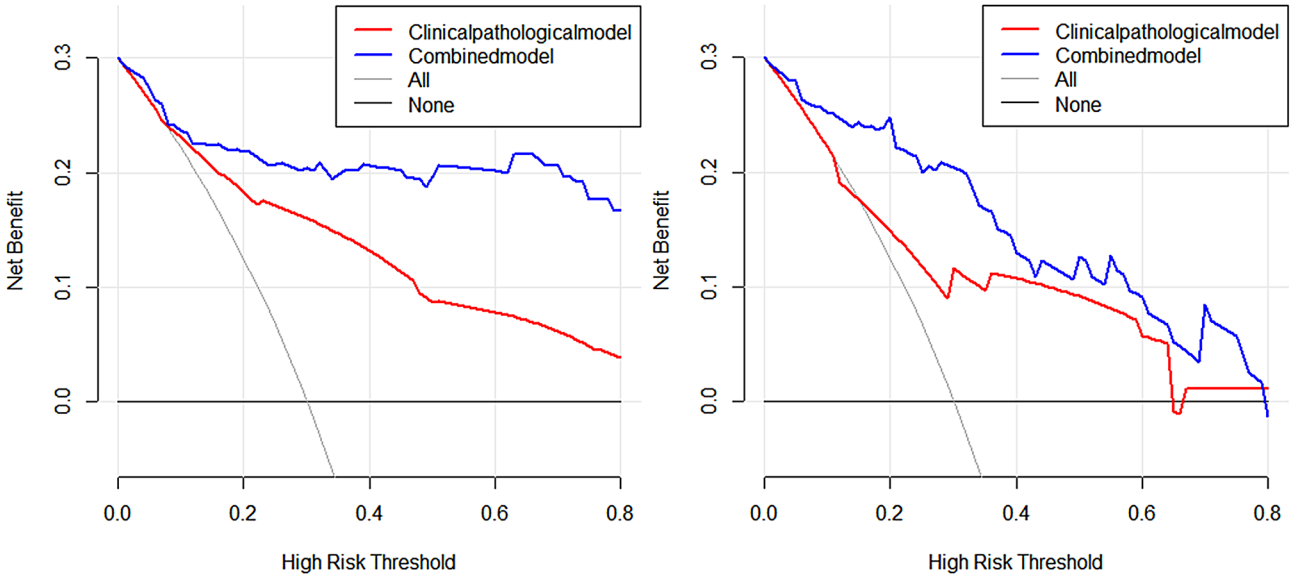

Fig. 5 The decision curve in this study confirmed that the combined model had a higher clinical net benefit in both the training set (left) and the test set (right)

Nevertheless, BG remains one of the most prevalent intracranial malignancies, accounting for up to 50% of primary brain tumors, and is generally associated with poor prognosis. While the etiology of BG remains controversial within the medical community, accumulating evidence suggests strong correlations with genetic mutations, environmental pollution, and electromagnetic radiation. Notably, BG incidence shows no significant demographic disparities across populations [16, 17]. Current therapeutic strategies for BG include craniotomy, Da Vinci robotic-assisted neuroendoscopic minimally invasive surgery, radiotherapy, chemotherapy, and targeted therapies. These approaches aim to maximize tumor resection while controlling neoplastic growth and dissemination. However, BG exhibits marked heterogeneity, resulting in interpatient variability in tumor characteristics, progression rates, and treatment responses. Consequently, many patients face recurrence risks post-treatment, with recurrent tumors being more refractory to management, incurring higher costs, and exposing

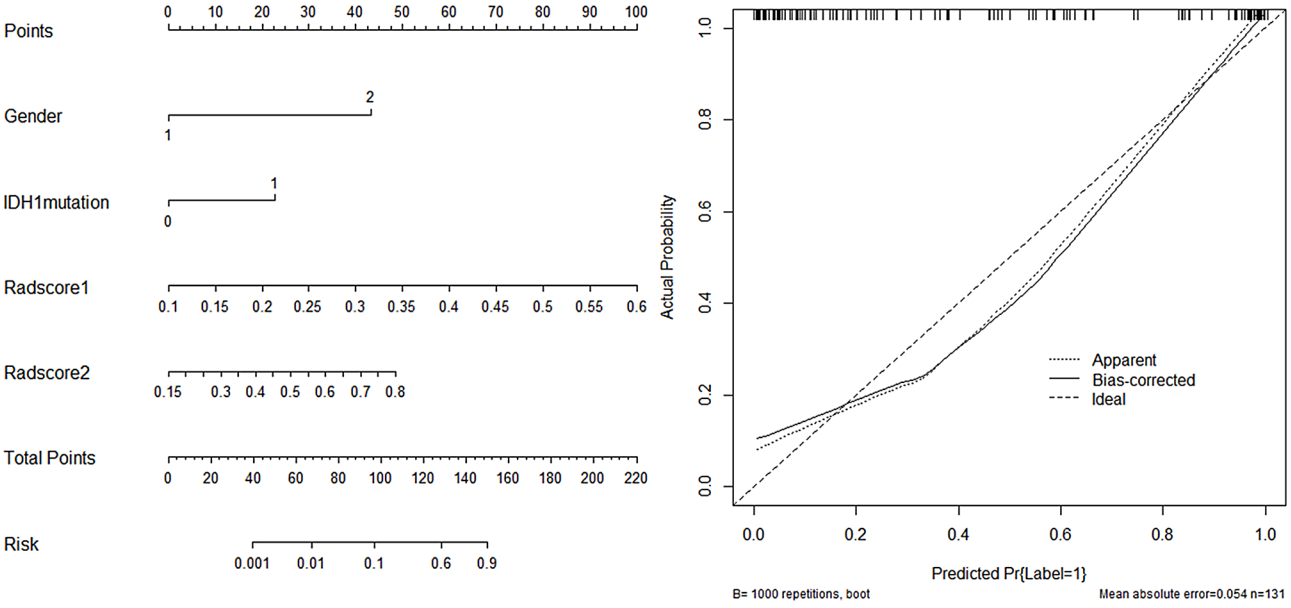

Fig. 6 The nomogram (left figure) and calibration curve (right figure) developed based on the combined model had achieved good benefits in clinically predicting BG recurrence

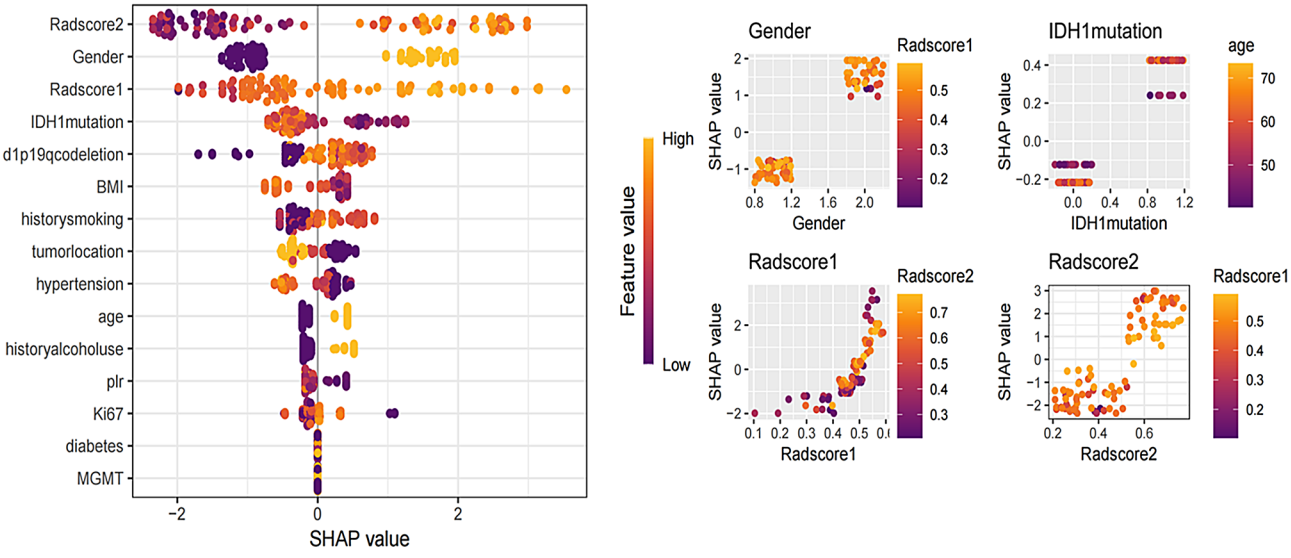

Fig. 7 The SHAP values output by the XGBoost algorithm model confirmed that factors such as gender, IDH1 mutation, Radscore 1, and Radscore 2 were important influencers for predicting BG recurrence, which was consistent with our research. Red represents lower values, while yellow represents higher values

Table 5 Univariate and multivariate Cox regression analysis of clinical and radiomic predictors for BG survival

Factors	Classification	All	HR (univariable)	HR (multivariable)
Gender	Male	121 (64.7)	-	-
	Female	66 (35.3)	3.17 (2.06–4.87, $p < 0.001$)	3.33 (2.08–5.33, $p < 0.001$)
IDH1mutation	Yes	108 (57.8)	-	-
	No	79 (42.2)	1.59 (1.04–2.42, $p = 0.031$)	2.47 (1.58–3.87, $p < 0.001$)
Radscore1	Mean (SD)	0.5 (0.1)	4414.94 (115.88-168210.91, $p < 0.001$)	756.32 (21.15-27043.48, $p < 0.001$)
Radscore2	Mean (SD)	0.5 (0.2)	180.13 (43.64-743.56, $p < 0.001$)	71.19 (16.88-300.21, $p < 0.001$)

P-value < 0.05* indicates statistical significance, both univariate and multivariate Cox regression analyses confirmed that gender, IDH1 mutation, Radscore 1, and Radscore 2 serve as independent risk factors for survival outcomes in brain glioma (BG) patients ($p < 0.001$)

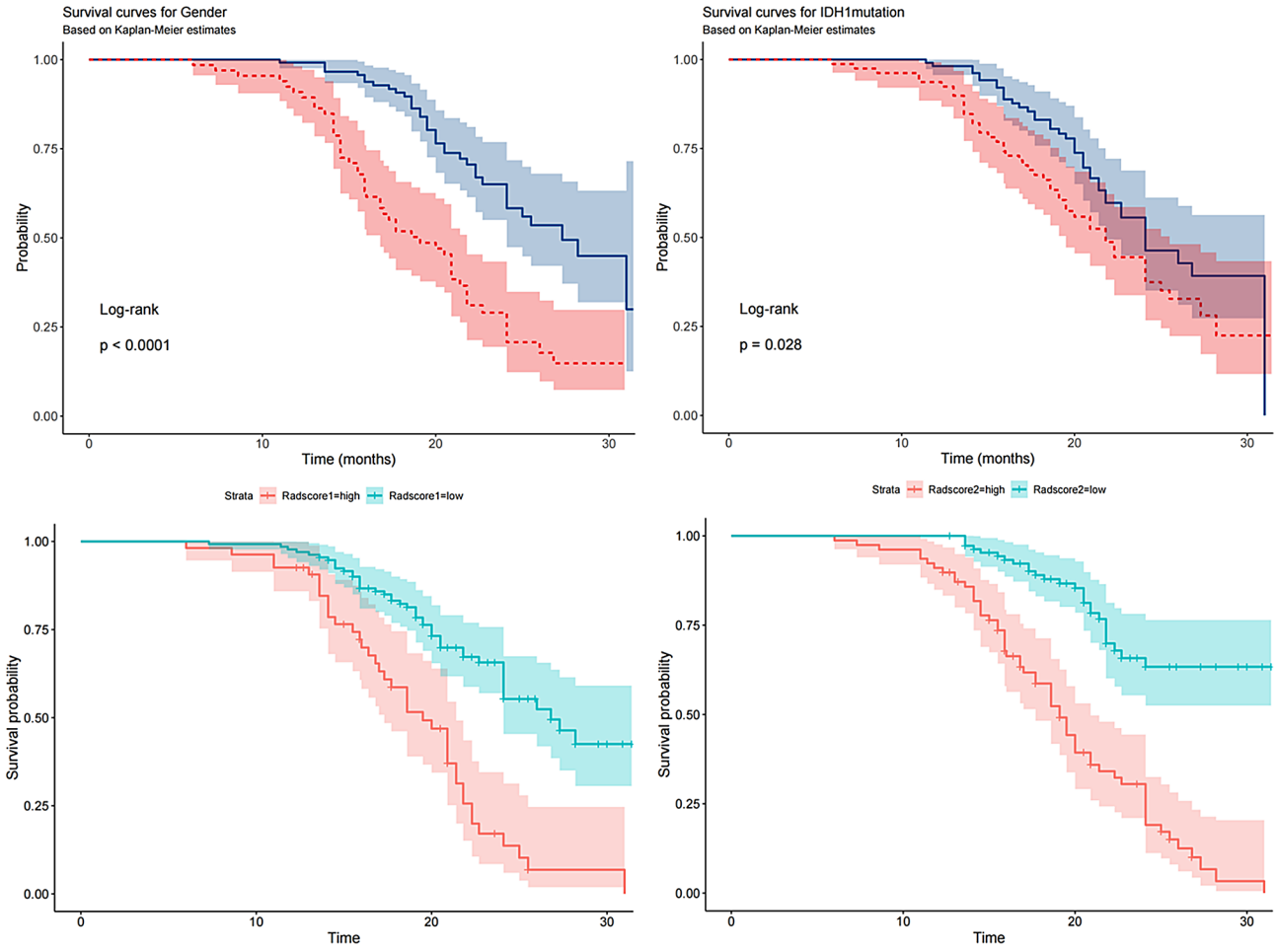

Fig. 8 KM analysis confirmed that IDH1 mutations, gender, and Delta habitat radscore1/2 were factors influencing BG survival

patients to additional mortality from extensive radiotherapy. This underscores the critical need for biomarkers enabling early prediction of postoperative recurrence. Our study focused on peritumoral habitats—regions surrounding the resection cavity where recurrence is most frequent—by extracting preoperative radiomic features from both the tumor core and its periphery (3–12 mm margin). We developed a predictive model for 3-year postoperative recurrence, providing a framework for personalized treatment planning and prognostic stratification [18, 19].

Key Determinants of Recurrence: Significant differences were observed between recurrent and non-recurrent cohorts in gender, IDH1 mutation status, 1p19q co-deletion, MRI enhancement patterns, and delta habitat radiomic scores (Radscore1: peritumoral; Radscore2: intratumoral). These factors collectively influence recurrence risk through distinct mechanisms: (1) Sex Differences: In clinical practice, adjuvant chemoradiotherapy is a conventional treatment for patients with positive surgical margins on pathological examination after BG surgery. However, female patients demonstrated higher recurrence susceptibility in this study, potentially attributable to lower radiotherapy tolerance and increased postoperative complications (e.g., alopecia, neurofunctional decline, immunosuppression), which may indirectly exacerbate recurrence risks. (2) IDH1 Mutations: Wild-type IDH1 diffuse astrocytomas exhibit greater malignant transformation potential, chemoresistance, and poorer outcomes, whereas IDH1-mutant tumors correlate with favorable temozolomide sensitivity and prolonged survival. (3) 1p19q Co-Deletion: This molecular hallmark of oligodendroglioma suppresses tumor growth kinetics and metastatic propensity, conferring a relatively indolent clinical course [20–23]. (4) MRI Enhancement Patterns: Inflow Pattern (Gradual Enhancement, benign/well-differentiated tumors): Characterized by rapid signal intensity elevation followed by gradual stabilization. This reflects progressive blood flow increase within the lesion, typically associated with benign neoplasms. The sustained plateau suggests adequate vascular supply without significant contrast washout. Plateau Pattern (Persistent Enhancement, borderline/low-grade malignancies): Demonstrates rapid signal peak attainment

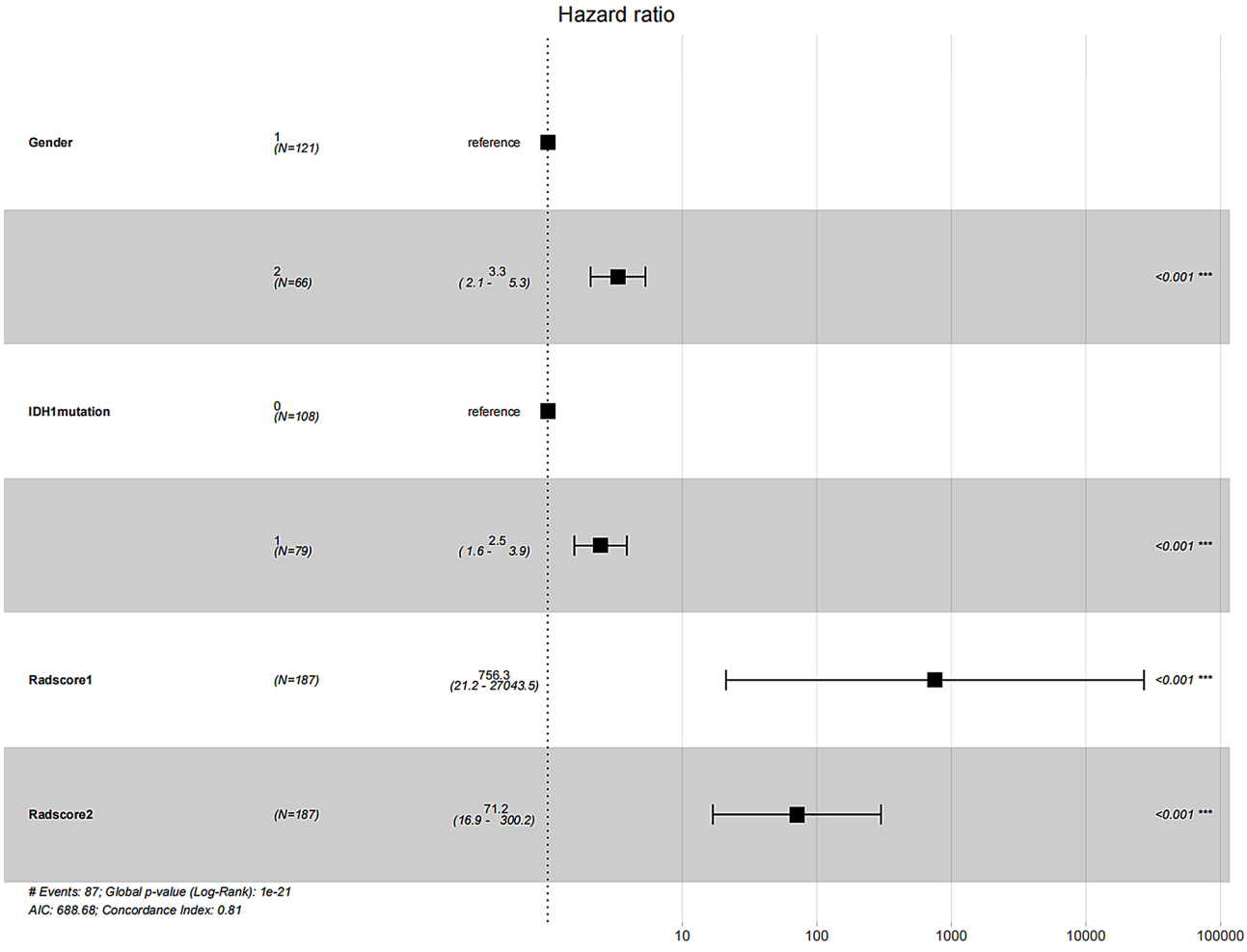

Fig. 9 The forest plot derived from Cox regression analysis demonstrated that both radscore1 and radscore2 in the BG cohort serve as significant predictors of survival outcomes

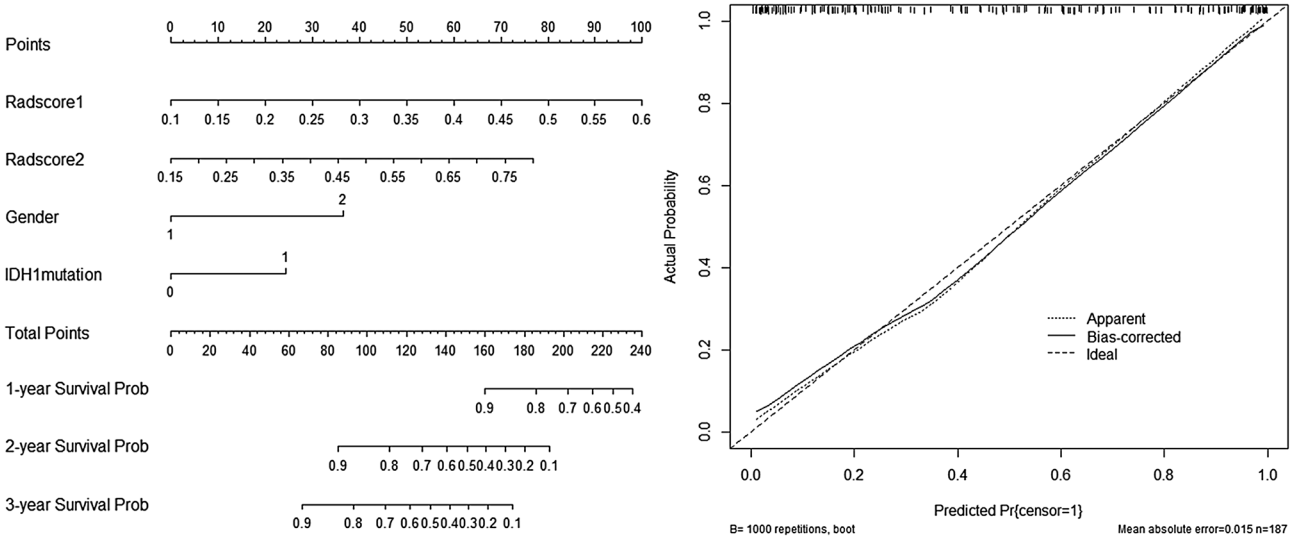

Fig. 10 The nomogram for survival established based on these factors(IDH1 mutations, gender, and Radscore1/2 also holds certain clinical value

with subsequent maintenance of enhancement intensity. This hemodynamic profile indicates both rich vascularization and effective contrast retention, commonly observed in hypervascular benign tumors (e.g., hepatocellular adenoma) or borderline/low-grade malignant lesions (e.g., well-differentiated neuroendocrine tumors). Washout Pattern (Rapid Washout, high-grade aggressive tumors): Exhibits swift signal amplification during arterial phase followed by precipitous decline in venous/delayed phases. This "fast-in-fast-out" phenomenon correlates with hypermetabolic malignancies demonstrating aggressive angiogenesis and enhanced interstitial permeability, typically seen in high-grade carcinomas (e.g., HCC, cholangiocarcinoma) and metastatic lesions. These enhancement patterns not only serve as critical diagnostic classifiers for tumor characterization but also carry significant prognostic implications. The washout pattern particularly correlates with advanced histological grades, increased mitotic activity, and poorer clinical outcomes, while plateau-type enhancement often indicates indolent biological behavior. Current evidence suggests these dynamic patterns reflect underlying tumor microvascular architecture and endothelial permeability characteristics, providing non-invasive biomarkers for both diagnostic classification and prognostic stratification [24, 25].

Radiomics, introduced by Lambin et al. in 2012, has emerged as a transformative tool in medical imaging, enabling non-invasive, dynamic characterization of tumor biology by extracting high-dimensional features from regions of interest (ROIs). In this study, we focused on contrast-enhanced T1-weighted imaging (CE-T1WI) to quantify intratumoral and peritumoral habitats in brain gliomas (BGs). Our methodology not only delineated hemodynamic changes and microenvironmental dynamics but also captured intrinsic tumor biology, demonstrating robust predictive power for postoperative recurrence. Guided by neuroimaging consensus protocols, ROIs were segmented along peritumoral hyperintense regions (3–12 mm margins) on CE-T1WI. Subsequent pixel resampling ($1 \times 1 \times 1$ mm^3) and Z-score normalization minimized voxel size dependency and interindividual variability. Key radiomic features included Maximum2DDiameterColumn and Skewness were integrated into radiomics scores (Radscore): Maximum2DDiameterColumn (reflecting the maximum 3D pixel intensity) inversely correlated with recurrence risk ($P < 0.05$). Elevated values, potentially influenced by hemorrhage, necrosis, or vascular integrity, may indicate less aggressive phenotypes. Skewness (measuring pixel value asymmetry) positively correlated with recurrence ($P < 0.01$). Higher skewness reflects increased tissue heterogeneity, likely driven by disorganized cellular architecture and poor prognosis [26–28]. Intratumoral vs. Peritumoral Radiomics, Our dual-habitat analysis revealed distinct biological insights: 1.Intratumoral Region(Radscore2): Features such as GrayLevelNonUniformity and SizeZoneNonUniformityNormalized quantified cellular heterogeneity, including treatment-resistant glioma stem cells and intratumoral microglia that drive tumor progression. 2. Peritumoral Habitat (Radscore1): Parameters like Maximum2DDiameterColumn and Skewness captured invasive traits, such as VEGF-driven angiogenesis and plasma leakage from disrupted capillaries, fostering tumor cell infiltration. Delta habitat radiomics outperformed static models by integrating peritumoral invasiveness metrics (Radscore1) with intratumoral heterogeneity (Radscore2). This dual-habitat approach improved predictive accuracy by 5.1–11.31% (AUC comparison:0.843.VS.0.802, 0.827.VS.0.743;) compared to single-region models, aligning with recent evidence that tumor-host interface dynamics drive recurrence. These hypoxic, hypervascular microenvironments significantly contribute to recurrence [29, 30]. Model Performance, The combined model (integrating radiomic scores with clinical variables) achieved superior predictive accuracy for recurrence (training AUC: 0.921; test AUC: 0.891), outperforming standalone clinicopathological or imaging models. Decision curve analysis confirmed its enhanced clinical net benefit. Kaplan-Meier analysis further identified IDH1 mutations and Radscore1/2 as independent survival predictors ($P < 0.01$), validated by XGBoost machine learning. These findings align with evidence that IDH1-wildtype gliomas exhibit aggressive biology and temozolomide resistance [27, 29, 31].I have included a real-world example to validate the usefulness of the nomogram. It concerns an external patient, ID 511, who is a female (44 points), with IDH1 wild-type (25 points), a radscore1 of 0.5 (80 points), and a radscore2 of 0.55 (30 points), totaling 179 points. The nomogram predicts a recurrence probability of > 0.9, which is consistent with the clinical outcome (recurrence after 17 months).

Limitations

While our study achieved methodological rigor, certain limitations warrant consideration. The restricted sample size precluded detection of significant MGMT methylation status differences between groups, despite observed variations in chemo-radiotherapy sensitivity. Future investigations should prioritize MGMT-stratified cohort expansion to elucidate its prognostic implications. Although our machine learning framework demonstrated clinical utility, performance optimization through advanced deep learning architectures and expanded clinical variable incorporation remains essential for enhanced predictive accuracy. Certainly, the lack of a certain proportion of external validation set poses a limitation in this study, which may affect the generalization performance of the model. In the future, we will

conduct multi-center research to enhance the predictive performance of the model.While data from multiple campuses improved internal validity, true external validation requires multi-center cohorts. Our ongoing collaboration with 5 institutions will test generalizability across diverse populations and MRI vendors (Philips, GE, Siemens) [32, 33].

Conclusion

Our delta habitat radiomics model, combining intratumoral/peritumoral biomarkers with clinicopathological variables, provides a robust tool for early recurrence prediction (≤ 3 years post-surgery) and survival stratification in BG patients. Key indicators included IDH1 mutation status and Radscore1/2 offer actionable insights for personalized therapeutic strategies and postoperative surveillance. This paradigm advances precision neuro-oncology, bridging the gap between imaging biomarkers and clinical decision-making.

Acknowledgements
This study was supported by the Graduate Education Research Project Fund of Hubei University of Medicine (YJ2022013) and the Xiangyang Science and Technology Plan Key Project Fund (2022YL34A).

Author contributions
Li.Song. and Zhang. wrote the main manuscript text and Ji.Song. prepared figures. All authors reviewed the manuscript.

Funding
General Program of the Natural Science Foundation of Hubei Province (Exploring the Prediction of Immunophenotyping and Prognosis Modeling for Oropharyngeal Cancer through Multi-modality Imaging-Pathomics Combined with Generalized Machine Learning– JCZRYB202501213-belonged to Peng An). Innovative Research Program of Xiangyang No.1 People's Hospital (XYY2025QN16 and XYY2025SD17), and the "323" Public Health Project of the Hubei Health Commission and the Xiangyang No.1 People's Hospital (XYY2022-323).

Data availability
https://pan.baidu.com/s/1KVfvWtLuWUcSXWypDzKTbg?pwd=wuwz.

Declarations

Human ethics and consent to participate declarations
The experimental protocol was formulated in accordance with the ethical guidelines of the Declaration of Helsinki and approved by the Human Ethics Committee of Xiangyang No.1 People's Hospital affiliated with Hubei University of Medicine (Issue No. XYYYE20240011).

Patient consent
Written informed consent was obtained from the participants or their guardians.

Consent for publication
All authors and participants have agreed to the publication of the results of this study.

Competing interests
The authors declare no competing interests.

Author details
[1]Department of Oncology, Surgery and Radiology, Xiangyang No. 1 People's Hospital, Hubei University of Medicine, Xiangyang 441000, China
[2]Department of Internal Medicine, Pathology and Epidemiology, Xiangyang Key Laboratory of Maternal-Fetal Medicine on Fetal Congenital Heart Disease, Xiangyang No. 1 People's Hospital, Hubei University of Medicine, Hubei, P.R.C, Xiangyang, Hubei Province 441000, China

Received: 24 November 2024 / Accepted: 17 March 2025
Published online: 28 March 2025

References

1. Omuro A, Brandes AA, Carpentier AF, et al. Radiotherapy combined with nivolumab or Temozolomide for newly diagnosed glioblastoma with unmethylated MGMT promoter: an international randomized phase III trial. Neuro Oncol. 2023;25(1):123–34. https://doi.org/10.1093/neuonc/noac099.
2. Kunimatsu A, Yasaka K, Akai H, Sugawara H, Kunimatsu N, Abe O. Texture analysis in brain tumor MR imaging. Magn Reson Med Sci. 2022;21(1):95–109. https://doi.org/10.2463/mrms.rev.2020-0159.
3. Prasanna P, Patel J, Partovi S, Madabhushi A, Tiwari P. Radiomic features from the peritumoral brain parenchyma on treatment-naïve multi-parametric MR imaging predict long versus short-term survival in glioblastoma multiforme: preliminary findings [published correction appears in Eur radiol. 2017;27(10):4198–4199. Doi: https://doi.org/10.1007/s00330-017-4815-y]. Eur Radiol. 2017;27(10):4188–97. https://doi.org/10.1007/s00330-016-4637-3.
4. Chougule T, Gupta RK, Saini J, et al. Radiomics signature for Temporal evolution and recurrence patterns of glioblastoma using multimodal magnetic resonance imaging. NMR Biomed. 2022;35(3):e4647. https://doi.org/10.1002/nbm.4647.
5. Geraghty BJ, Dasgupta A, Sandhu M, et al. Predicting survival in patients with glioblastoma using MRI radiomic features extracted from radiation planning volumes. J Neurooncol. 2022;156(3):579–88. https://doi.org/10.1007/s11060-021-03939-9.
6. Aftab K, Aamir FB, Mallick S, et al. Radiomics for precision medicine in glioblastoma. J Neurooncol. 2022;156(2):217–31. https://doi.org/10.1007/s11060-021-03933-1.
7. Lopez CJ, Nagornaya N, Parra NA, et al. Association of radiomics and metabolic tumor volumes in radiation treatment of glioblastoma multiforme. Int J Radiat Oncol Biol Phys. 2017;97(3):586–95. https://doi.org/10.1016/j.ijrobp.2016.11.011.
8. Mărginean L, Ştefan Ş, A P, Lebovici, et al. CT in the differentiation of gliomas from brain metastases: the radiomics analysis of the peritumoral zone. Brain Sci. 2022;12(1):109. https://doi.org/10.3390/brainsci12010109. Published 2022 Jan 14.
9. 9.Zhou H, Vallières M, Bai HX et al. MRI features predict survival and molecular markers in diffuse lower-grade gliomas [published correction appears in Neuro Oncol. 2017;19(12):1701. doi: https://doi.org/10.1093/neuonc/nox110]. Neuro Oncol. 2017;19(6):862–870. https://doi.org/10.1093/neuonc/now256
10. Antunes JT, Ismail M, Hossain I, et al. RADIomic Spatial textural descriptor (RADISTAT): quantifying Spatial organization of imaging heterogeneity associated with tumor response to treatment. IEEE J Biomed Health Inf. 2022;26(6):2627–36. https://doi.org/10.1109/JBHI.2022.3146778.
11. Qin JB, Liu Z, Zhang H, et al. Grading of gliomas by using radiomic features on multiple magnetic resonance imaging (MRI) sequences. Med Sci Monit. 2017;23:2168–78. https://doi.org/10.12659/msm.901270. Published 2017 May 7.
12. Ismail M, Prasanna P, Bera K, et al. Radiomic deformation and textural heterogeneity (R-DepTH) descriptor to characterize tumor field effect: application to survival prediction in glioblastoma. IEEE Trans Med Imaging. 2022;41(7):1764–77. https://doi.org/10.1109/TMI.2022.3148780.
13. Corr F, Grimm D, Saß B et al. Radiogenomic Predictors of Recurrence in Glioblastoma-A Systematic Review. J Pers Med. 2022;12(3):402. Published 2022 Mar 4. https://doi.org/10.3390/jpm12030402
14. Li Z, Wang Y, Yu J, Guo Y, Cao W. Deep learning based radiomics (DLR) and its usage in noninvasive IDH1 prediction for low grade glioma. Sci Rep. 2017;7(1):5467. https://doi.org/10.1038/s41598-017-05848-2. Published 2017 Jul 14.
15. Zhang H, Zhang B, Pan W, et al. Preoperative Contrast-Enhanced MRI in differentiating glioblastoma from Low-Grade gliomas in the cancer imaging archive database: A Proof-of-Concept study. Front Oncol. 2022;11:761359. https://doi.org/10.3389/fonc.2021.761359. Published 2022 Jan 17.

16. Lao J, Chen Y, Li ZC, et al. A deep Learning-Based radiomics model for prediction of survival in glioblastoma multiforme. Sci Rep. 2017;7(1):10353. https://doi.org/10.1038/s41598-017-10649-8. Published 2017 Sep 4.
17. Jia X, Zhai Y, Song D, et al. A multiparametric MRI-Based radiomics nomogram for preoperative prediction of survival stratification in glioblastoma patients with standard treatment. Front Oncol. 2022;12:758622. https://doi.org/10.3389/fonc.2022.758622. Published 2022 Feb 16.
18. Gore S, Chougule T, Jagtap J, Saini J, Ingalhalikar M. A review of radiomics and deep predictive modeling in glioma characterization. Acad Radiol. 2021;28(11):1599–621. https://doi.org/10.1016/j.acra.2020.06.016.
19. Luo H, Zhuang Q, Wang Y et al. A novel image signature-based radiomics method to achieve precise diagnosis and prognostic stratification of gliomas. lab invest. 2021;101(4):450–62. https://doi.org/10.1038/s41374-020-0472-x
20. Matteoni S, Abbruzzese C, Villani V, et al. The influence of patient sex on clinical approaches to malignant glioma. Cancer Lett. 2020;468:41–7. https://doi.org/10.1016/j.canlet.2019.10.012.
21. Choi Y, Nam Y, Jang J, et al. Radiomics May increase the prognostic value for survival in glioblastoma patients when combined with conventional clinical and genetic prognostic models. Eur Radiol. 2021;31(4):2084–93. https://doi.org/10.1007/s00330-020-07335-1.
22. Cheng J, Liu J, Yue H, Bai H, Pan Y, Wang J. Prediction of glioma grade using intratumoral and peritumoral radiomic features from multiparametric MRI images. IEEE/ACM Trans Comput Biol Bioinform. 2022;19(2):1084–95. https://doi.org/10.1109/TCBB.2020.3033538.
23. Park JE, Ham S, Kim HS, et al. Diffusion and perfusion MRI radiomics obtained from deep learning segmentation provides reproducible and comparable diagnostic model to human in post-treatment glioblastoma. Eur Radiol. 2021;31(5):3127–37. https://doi.org/10.1007/s00330-020-07414-3.
24. Bhandari AP, Liong R, Koppen J, Murthy SV, Lasocki A. Noninvasive determination of IDH and 1p19q status of Lower-grade gliomas using MRI radiomics: A systematic review. AJNR Am J Neuroradiol. 2021;42(1):94–101. https://doi.org/10.3174/ajnr.A6875.
25. Han Y, Yang Y, Shi ZS, et al. Distinguishing brain inflammation from grade II glioma in population without contrast enhancement: a radiomics analysis based on conventional MRI. Eur J Radiol. 2021;134:109467. https://doi.org/10.1016/j.ejrad.2020.109467.
26. Pinto Dos Santos D, Garcia Santos JM. Radiomics for prediction of survival in lower-grade gliomas-it's time to move beyond the crystal ball. Eur Radiol. 2021;31(4):1783–4. https://doi.org/10.1007/s00330-020-07603-0.
27. Zhang S, Sun H, Su X, et al. Automated machine learning to predict the co-occurrence of isocitrate dehydrogenase mutations and O6 -methylguanine-DNA methyltransferase promoter methylation in patients with gliomas. J Magn Reson Imaging. 2021;54(1):197–205. https://doi.org/10.1002/jmri.27498.
28. Wang J, Zheng X, Zhang J, et al. An MRI-based radiomics signature as a pretreatment noninvasive predictor of overall survival and chemotherapeutic benefits in lower-grade gliomas. Eur Radiol. 2021;31(4):1785–94. https://doi.org/10.1007/s00330-020-07581-3.
29. Kim AR, Choi KS, Kim MS, et al. Absolute quantification of tumor-infiltrating immune cells in high-grade glioma identifies prognostic and radiomics values. Cancer Immunol Immunother. 2021;70(7):1995–2008. https://doi.org/10.1007/s00262-020-02836-w.
30. Kaur G, Rana PS, Arora V. State-of-the-art techniques using pre-operative brain MRI scans for survival prediction of glioblastoma multiforme patients and future research directions. Clin Transl Imaging. 2022;10(4):355–89. https://doi.org/10.1007/s40336-022-00487-8.
31. Sun YZ, Yan LF, Han Y et al. Differentiation of Pseudoprogression from True Progressionin Glioblastoma Patients after Standard Treatment: A Machine Learning Strategy Combinedwith Radiomics Features from T1-weighted Contrast-enhanced Imaging. BMC Med Imaging. 2021;21(1):17. Published 2021 Feb 3. https://doi.org/10.1186/s12880-020-00545-5
32. Le NQK, Hung TNK, Do DT, Lam LHT, Dang LH, Huynh TT. Radiomics-based machine learning model for efficiently classifying transcriptome subtypes in glioblastoma patients from MRI. Comput Biol Med. 2021;132:104320. https://doi.org/10.1016/j.compbiomed.2021.104320.
33. Sartoretti E, Sartoretti T, Wyss M, et al. Amide proton transfer weighted (APTw) imaging based radiomics allows for the differentiation of gliomas from metastases. Sci Rep. 2021;11(1):5506. https://doi.org/10.1038/s41598-021-85168-8. Published 2021 Mar 9.

Publisher's note